

Article ID: 1001-3555(2023)06-0523-05

One-pot Synthesis of WS₂/WO₃ Heterojunction for UV-Visible-light-driven CO₂ Reduction to CO

DU Min-xing^{1,2}, SUN Yu-xia¹, YAN Chang-zeng^{1*}, LI Yue-hui^{1*}

(1. State Key Laboratory for Oxo Synthesis and Selective Oxidation, Lanzhou Institute of Chemical Physics, Chinese Academy of Sciences, Lanzhou 730000, China; 2. University of Chinese Academy of Sciences, Beijing 100049, China)

Abstract: Photocatalytic reduction of CO₂ to produce energy-rich hydrocarbons without sacrificing reagents is of great significance. Here, the 1T/2H-WS₂/WO₃ heterojunction catalyst is prepared by one-pot hydrothermal method, which shows a prominent CO₂ reduction performance with water as an electron donor, affording CO as the sole carbonaceous product at a production rate of 3.87 μmol·g⁻¹·h⁻¹ under visible light. Moreover, under UV-visible light irradiation, the 1T/2H-WS₂/WO₃ photocatalyst shows better catalytic activity and 34.39 μmol·g⁻¹·h⁻¹ yield of CO. Importantly, the stability test shows no distinctive performance degradation even after 64 h reaction. This work provides new insight for designing and fabricating semiconductor heterojunction photocatalysts with high efficiency for solar-energy conversion.

Key words: one-pot synthesis; WS₂/WO₃ heterojunction; CO₂ reduction; no sacrifice reagent; UV-Visible light

CLC number: O643.32

Document code: A

DOI: 10.16084/j.issn1001-3555.2023.06.001

Photoreduction of CO₂ into energy-rich molecules (e.g., CO, CH₃OH, CH₄, C₂H₅OH, and C₂H₆) provides a sustainable way of CO₂ utilization^[1-4]. Numerous efforts have been devoted to design of different photocatalysts over the past decades. One of the most effective strategies is to rationally tailor bi- or multifunctional semiconductor homo/heterojunctions^[5-6].

WS₂ is a typical type of group-VI transition-metal dichalcogenide, where the individual S-W-S atomic planes bonded through Van der Waals forces^[6]. WS₂ photocatalyst has received particular research interests due to its tunable bandgap, wide light absorption range and excellent charge mobility properties^[7]. Theoretically, it has been predicted that WS₂ layers have two distinct symmetries depending on the arrangement manner of S atoms, i.e., hexagonal close packing and trigonal prismatic coordination phase (2H) or the tetragonal symmetry and octahedral coordination phase (1T)^[8]. Notably, thermodynamically stable 2H-WS₂ is suitable to form heterojunctions with other semiconductors for CO₂ photoreduction. And the 1T-WS₂ has suitable metal conductivity and plenty of active sites on the base plane and the edge areas, which could effectively transfer the electrons and thus acts as co-catalyst for CO₂ reduction. Interestingly, 1T/2H-WS₂ homojunctions can be formed by partial oxidation of metastable 1T-WS₂, enabling facile heterojunctions construction by integrating with other band structure-matching semiconductor materials^[9].

Herein, a novel heterojunction photocatalyst was prepared by integrating multiphase 1T/2H-WS₂ homojunction with WO₃ via one-pot hydrothermal treatment. Specifically, 1T/2H-WS₂/

WO₃ showed excellent catalytic performance for CO₂ photoreduction using water vapor as electron donor, affording CO as the sole carbonaceous product with a production rate of 3.87 μmol·g⁻¹·h⁻¹ under visible light irradiation. Besides, under UV-visible light irradiation, the 1T/2H-WS₂/WO₃ photocatalyst showed higher rate of CO as 34.39 μmol·g⁻¹·h⁻¹. In addition, it exhibited excellent stability under photoreduction conditions. The formed heterostructure in 1T/2H-WS₂/WO₃ ensures a multi-step and cascade transfer pathway of photogenerated electrons, which facilitates accumulation of electrons on 1T-WS₂ for the photocatalytic CO₂ reduction and subsequently improves the selectivity of CO. This work provides new insight for designing and fabricating high-efficiency photo-active semiconductor-based photocatalysis for CO₂ utilization.

1 Experimental section

Synthesis of catalysts. One-pot hydrothermal method was adopted to prepare the 1T/2H-WS₂/WO₃ materials. 1.19 g (3 mmol) WCl₆ and 2.28 g (30 mmol) thioacetamide were dispersed in 40 mL DI water, and further stirred for 60 min. The obtained mixture was transferred into the 50 mL Teflon lined hydrothermal reactor and heated at 260 °C for 24 h. After cooling to room temperature, the product was collected by centrifugation at 8 000 r·min⁻¹, and washed thoroughly with ethanol and DI water. The product was vacuum dried overnight at 60 °C.

Characterization. The Powder X-ray diffraction (XRD)

Received date: 2023-03-01; **Revised date:** 2023-03-30.

Foundation: The National Natural Science Foundation of China (Nos. 21633013 and 22102197) and CAS LICP Cooperative Fund of Collaborative Innovation Alliance for Young Scientists (HZJJ23-5).

Biography: Du Min-xing(1993-), male, doctor degree candidate, mainly engaged in research of photocatalysis, carbon dioxide conversion and utilization, E-mail: minxingdu@126.com.

* Corresponding authors. E-mail: yanchangzeng@163.com; yhli@licp.cas.cn.

patterns were obtained using a Rigaku SmartLab 3 kW diffractometer equipped with Cu K α radiation. UV-vis diffuse reflectance spectroscopy (DRS) spectra were measured by Shimadzu UV-2550 spectrophotometer with an integrating sphere attachment. The morphologies were examined by field emission scanning electron microscopy (FE-SEM, Hitachi, Regulus-8100) at an acceleration voltage of 5 kV. The specific surface area was determined by the Brunauer-Emmett-Teller (BET) method. The pore size was obtained using the desorption isotherm through the Barrett-Joyner-Halenda (BJH) method. HRTEM images were taken on JEOL JEM-2100F field-emission high-resolution transmission electron microscope operated at 200 kV. X-ray photoelectron spectroscopy (XPS) analysis was recorded on a thermoscientific NEXSA system, using monochromatic Al K α radiation (1486.6 eV).

Photocatalytic CO₂ reduction measurements. 15 mg of photocatalyst powder was carried out in a gas-closed system with a gas-circulated pump (EL-PAEM-D8 system, Beijing China Education Au-light Co., Ltd) equipped with a 300-W Xe lamp (PE300BUV, 200 ~ 780 nm). The 420 nm cutoff filter (420 nm < λ < 780 nm) was used to ensure that photocatalytic CO₂ reduction under visible light irradiation. During light irradiation, the gas products were analyzed by GC7920 with a

flame ionization detector (FID) and a thermal conductive detector (TCD).

Photocatalytic CO₂ stability test. To evaluate the stability of prepared catalysts, the photocatalytic reactor was thoroughly dried at 100 °C for 2 h, then, 15 mg of catalysts were maintained in this reaction cell. Subsequently, high-purity CO₂ gas and water were introduced into the degassed system for further photoreduction performance evolution under visible light irradiation. The same measurement process was repeated for 4 times.

Photocatalytic activity calculation. The photocatalytic reaction rate (R) for product rate ($\mu\text{mol}\cdot\text{g}^{-1}\cdot\text{h}^{-1}$) was calculated as follows:

$$R = \frac{n}{mt}$$

Where n refers to the number of moles of generated CO, m is the loading amount of catalyst (g), t is the irradiation time (h).

2 Results and discussion

The morphology of 1T/2H-WS₂/WO₃ heterostructures was measured using SEM technique. As shown in Fig.1(a), it displays typical flower-like microspheres morphology with the particle size of ~1 μm . The high-magnification SEM (Fig.1(b))

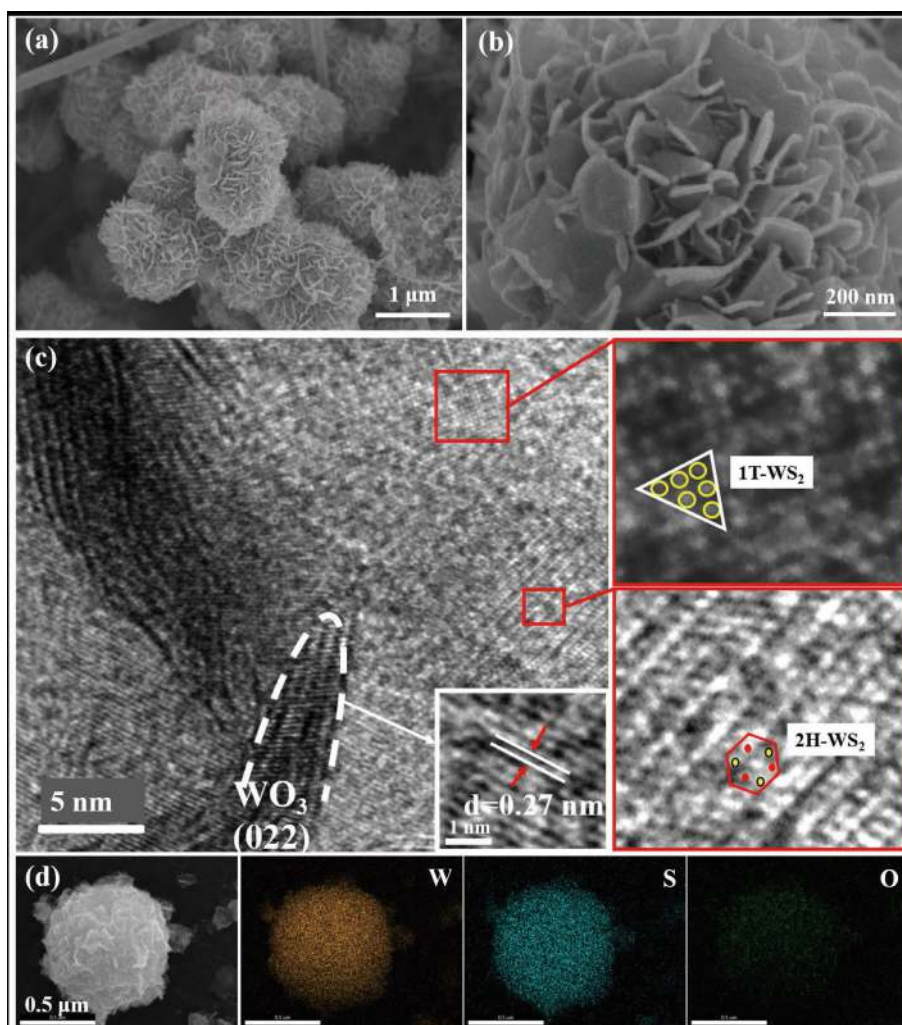


Fig.1 Morphology and chemical component analysis of the 1T/2H-WS₂/WO₃ sample
(a), (b) SEM images; (c) HRTEM image; (d) EDS elemental mapping

reveals that the flower-like microsphere was assembled by abundant nanoplates (~15 nm in thickness) as building blocks with highly branched structures. These congregated nanoplates create nanoscale 3D porous architecture on the exterior surface of WS₂, for faster CO₂ photoreduction. The microstructures of 1T/2H-WS₂/WO₃ were further investigated by the HRTEM (Fig. 1(c)). The lattice spacing of 0.27 nm corresponds to the plane of WO₃ (022). And the coexistence of the 1T-WS₂ and the 2H-WS₂ was confirmed. The compactly connected interface

between 1T-WS₂, 2H-WS₂ and WO₃ is conducive to rapid charge transfer. The EDX elemental mapping images (Fig. 1(d)) of the 1T/2H-WS₂/WO₃ heterostructure confirm the existence and W, S, and O distribution.

The XRD pattern of 1T/2H-WS₂/WO₃ is shown in Fig. 2(a). The diffraction peaks at 14.3°, 28.8°, 32.0°, 33.5°, 35.9°, 43.9°, 44.3° and 57.1° synchronized with the 2H-WS₂ (JCPDS No. 84-1398), assigning to (002), (004), (100), (101), (102), (006), (104), (008) planes, respectively. The peaks observed at

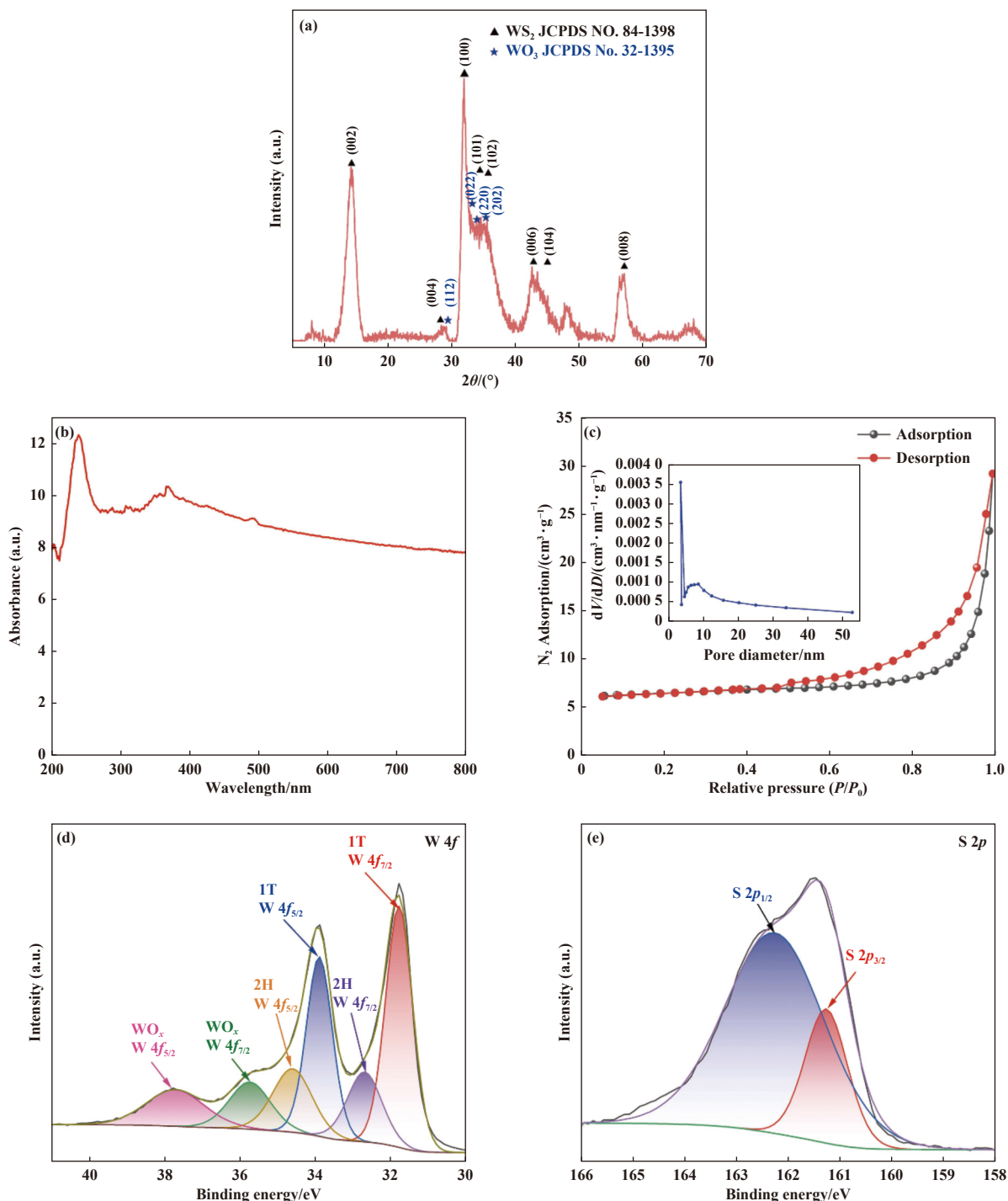


Fig.2 (a) XRD pattern; (b) UV-Vis DRS spectra (c) N₂ adsorption and desorption isotherms and BJH pore size distribution (inset); (d) W 4f and (e) S 2p XPS spectrum of 1T/2H-WS₂/WO₃

28.8°, 33.0°, 34.1° and 34.5° are associated with the (112), (022), (202), (220) planes of the triclinic WO_3 (JCPDS No. 32-1395)^[10].

The optical absorption characteristics of 1T/2H- WS_2/WO_3 were explored by UV-Vis DRS. As shown in Fig. 2(b), the 1T/2H- WS_2/WO_3 shows excellent visible light absorption, which can be attributed to the co-promotion of 1T- WS_2 and 2H- WS_2 ^[11]. As shown in Fig. 2(c), the BET surface area for 1T/2H- WS_2/WO_3 samples is $5 \text{ m}^2 \cdot \text{g}^{-1}$ and the pore volume is $0.03 \text{ cm}^3 \cdot \text{g}^{-1}$. The average pore size of the product based on the adsorption data is around 25.9 nm, which benefits the transports of CO_2 , gaseous H_2O and CO products.

XPS measurements were adopted to give insight into the chemical environment and element composition of the 1T/2H- WS_2/WO_3 heterostructure. As shown in Fig. 2(d), both 2H- WS_2 phase and 1T- WS_2 phase can be evidenced. 1T- WS_2 form is characterized by W 4f signal whose W 4f_{7/2} and 4f_{5/2} component are located at 31.8 and 33.9 eV. Two peaks at 32.7 and 34.6 eV are attributed to the W 4f_{7/2} and 4f_{5/2} of 2H- WS_2 ^[12]. The peaks located at 35.7 (W 4f_{7/2}) and 37.7 eV (W 4f_{5/2}) correspond to the W—O bond of WO_3 species^[8]. The characteristic peaks of both WS_2 and WO_3 can be clearly observed, which further confirms the successful synthesis of the WS_2/WO_3 heterostructure. Two distinct peaks in the S 2p spectrum also confirm the existence of WS_2 (Fig. 2(e)), the peaks located at 161.3 and 162.3 eV

belong to the S—W bond. These results demonstrate the successful formation of 1T/2H- WS_2/WO_3 heterostructures.

The photocatalytic activities of 1T/2H- WS_2/WO_3 for CO_2 reduction have been conducted and shown in Fig. 3(a) and 3(b). The dark reaction has been first explored before all tests, and only CO_2 signal can be observed in such a condition, which evidenced that there is no chemisorption of CO or O_2 on the photocatalyst surface. The 1T/2H- WS_2/WO_3 photocatalysts exhibited prominent and stable photocatalytic activities for CO_2 reduction into CO at a production rate of $3.87 \mu\text{mol} \cdot \text{g}^{-1} \cdot \text{h}^{-1}$ during 64 h test under visible light irradiation, under the irradiation of UV-visible light, the 1T/2H- WS_2/WO_3 photocatalysts shows better catalytic activity, and the yield of CO was $34 \mu\text{mol} \cdot \text{g}^{-1} \cdot \text{h}^{-1}$. O_2 was detected by GC, indicating that the photoinduced holes were utilized for oxidizing water to generate oxygen and hydrogen ions *via* the half-reaction ($2\text{H}_2\text{O} + 4\text{h}^+ \rightarrow \text{O}_2 + 4\text{H}^+$). For stability measurements, the 1T/2H- WS_2/WO_3 photocatalysts almost keep its original activity even after four cycles (Fig. 3(c) and 3(d), indicating that it can act as a stable photocatalyst for CO_2 reduction.

Based on our study and literature survey, we propose a possible reaction mechanism for 1T/2H- WS_2/WO_3 involved photocatalysis. Firstly, the formation of 2H- WS_2/WO_3 hetero-junction contributes to build an efficient cascade charge transfer channel, which enhances the separation of photogenerated

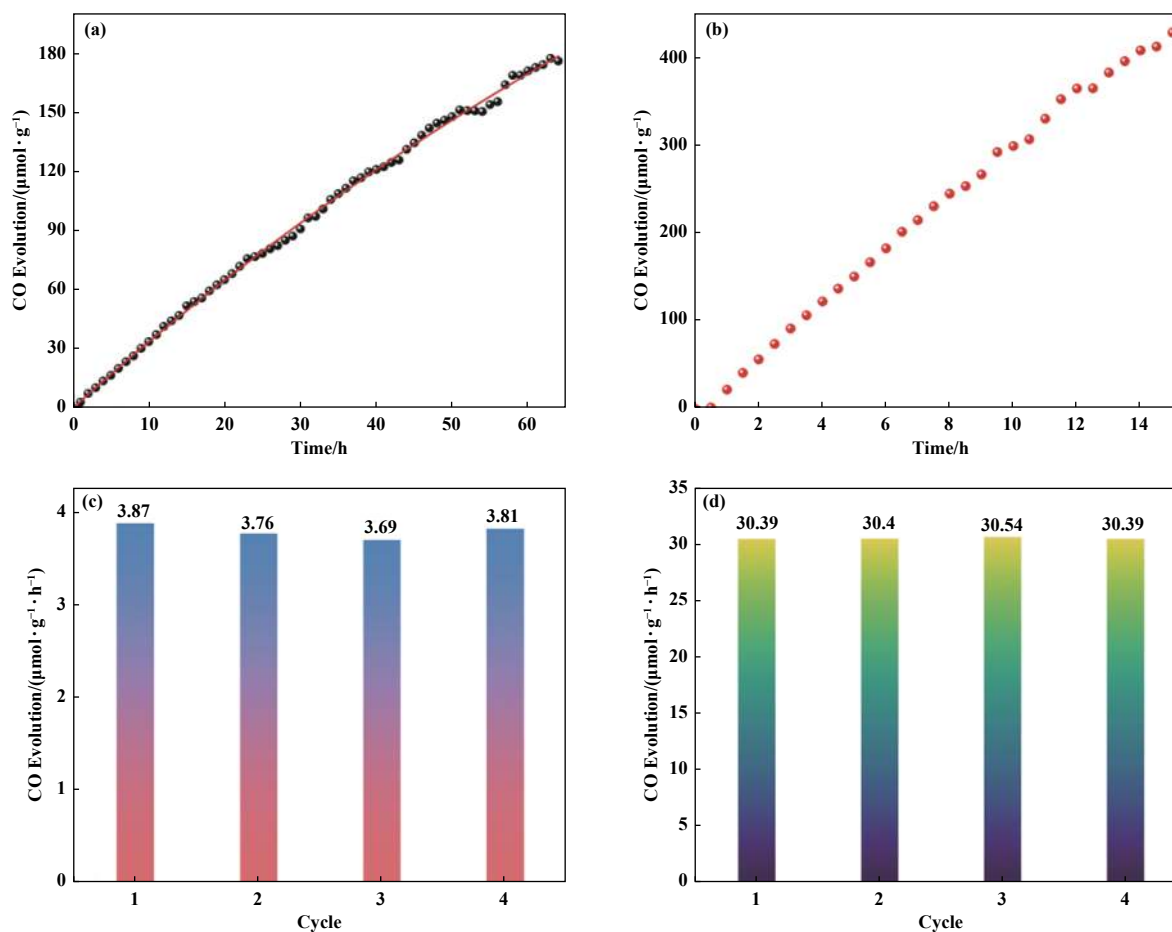


Fig.3 Time courses of photocatalytic CO evolution using 1T/2H- WS_2/WO_3 under visible light irradiation (a) and UV-Visible light irradiation (b); Average production rate of CO over 1T/2H- WS_2/WO_3 photocatalyst under visible light irradiation (c) and UV-Visible light irradiation (d) in photostability test

electron-hole pairs^[7,13]. Then, the charges are transferred to the surface of 1T-WS₂, which accelerates the separation of charges. Meanwhile, 1T-WS₂ plays a role as a co-catalyst, resulting in the high selectivity of CO generation^[9].

3 Conclusions

In conclusion, we successfully synthesized 1T/2H-WS₂/WO₃ heterostructures by one-pot hydrothermal method, which achieved photocatalytic reduction of CO₂ with H₂O, affording CO as the sole carbonaceous product with a production rate up to 3.87 μmol·g⁻¹·h⁻¹ under visible light irradiation, and 34.39 μmol·g⁻¹·h⁻¹ under UV-visible light irradiation. The formed heterostructures in the 1T/2H-WS₂/WO₃ have highly qualified contact interface, contributed to the fast charge separation and transfer. We expect that this research provides a valuable reference for designing and fabricating photocatalytically active semiconductor heterojunction with high efficiency for solar-energy conversion.

References

- [1] a. Wang H N, Zou Y H, Sun H X, *et al.* Recent progress and perspectives in heterogeneous photocatalytic CO₂ reduction through a solid-gas mode [J]. *Coordin Chem Rev*, 2021, **438**: 213906.
b. Liu Z, Wu Y L, Nie Y F, *et al.* Advances in the synthesis of CO₂-Based polycarbonate catalyzed by zinc glutarate[J]. *J Mol Catal (China)*, 2023, **37**(5): 498–511.
c. Ye Z, Luo H L, Jiang Z, *et al.* Recent advances of photocatalytic CO₂ overall reduction[J]. *J Mol Catal (China)*, 2023, **37**(2): 174–186.
- [2] a. Wang Y, Liu Y, Tao R, *et al.* Preparation and photocatalytic properties of K/Cl doped g-C₃N₄ [J]. *J Mol Catal (China)*, 2022, **36**(6): 561–570.
b. Tang W B, Zhang Z X, Chi J S, *et al.* The state of the art review on the photo-thermal reactor of CO₂ reduction[J]. *J Mol Catal (China)*, 2022, **36**(5): 499–512.
c. Song S J, Zhang X, Chen Y S, *et al.* Structural-activity relationship of Indium-based catalysts for CO₂ oxidative propane dehydrogenation[J]. *J Mol Catal (China)*, 2022, **36**(4): 338–346.
- [3] Dai C, Zhong L, Gong X, *et al.* Triphenylamine based conjugated microporous polymers for selective photoreduction of CO₂ to CO under visible light[J]. *Green Chem*, 2019, **21**: 6606–6610.
- [4] Yu X, Yang Z, Qiu B, *et al.* Eosin Y-functionalized conjugated organic polymers for visible-light-driven CO₂ reduction with H₂O to CO with high efficiency[J]. *Angew Chem Int Ed*, 2019, **58**: 632–636.
- [5] Mai H, Chen D, Tachibana Y, *et al.* Developing sustainable, high-performance perovskites in photocatalysis: Design strategies and applications[J]. *Chem Soc Rev*, 2021, **50**: 13692–13729.
- [6] Mortelmans W, Mehta A N, Balaji Y, *et al.* On the van der Waals epitaxy of homo-/heterostructures of transition metal dichalcogenides[J]. *ACS Appl Mater Interfaces*, 2020, **12**(24): 27508–27517.
- [7] Ma S, Zeng L, Tao L, *et al.* Enhanced photocatalytic activity of WS₂ film by laser drilling to produce porous WS₂/WO₃ heterostructure [J]. *Sci Rep*, 2017, **7**: 3125.
- [8] Scarfiello R, Mazzotta E, Altamura D, *et al.* An insight into chemistry and structure of colloidal 2D-WS₂ nanoflakes: Combined XPS and XRD study[J]. *Nanomaterials*, 2021, **11**(8): 1969.
- [9] Zhou Y, Ye Q, Shi X, *et al.* Regulating photocatalytic CO₂ reduction selectivity via steering cascade multi-step charge transfer pathways in 1T/2H-WS₂/TiO₂ heterojunctions [J]. *Chem Eng J*, 2022, **447**: 137485.
- [10] Liu X, Xu J, Cheng Z, *et al.* A sensitive acetone sensor based on WS₂/WO₃ nanosheets with *p-n* heterojunctions[J]. *ACS Appl Nano Mater*, 2022, **5**(9): 12592–12599.
- [11] Mahler B, Hoepfner V, Liao K, *et al.* Colloidal synthesis of 1T-WS₂ and 2H-WS₂ nanosheets: Applications for photocatalytic hydrogen evolution[J]. *J Am Chem Soc*, 2014, **136**(40): 14121–14127.
- [12] Toh R J, Mayorga-Martinez C C, Sofer Z, *et al.* 1T-phase WS₂ protein-based biosensor[J]. *Adv Funct Mater*, 2017, **27**: 1604923.
- [13] Lee N, Kwak J, Kwak J H, *et al.* Microwave-assisted evolution of WO₃ and WS₂/WO₃ hierarchical nanotrees[J]. *J Mater Chem A*, 2020, **8**: 9654–9660.

一锅法制备 1T/2H-WS₂/WO₃ 异质结用于紫外可见光催化的 CO₂ 还原

杜民兴^{1,2}, 孙玉霞¹, 闫长增^{1*}, 李跃辉^{1*}

(1. 中国科学院兰州化学物理研究所 羰基合成与选择氧化国家重点实验室, 甘肃 兰州 730000;

2. 中国科学院大学, 北京 100049)

摘要: 采用一锅水热法制备了 1T/2H-WS₂/WO₃ 异质结, 并利用 XRD、SEM、XPS 等对所制备的光催化材料进行了系统微结构表征。研究发现该异质结催化剂可用水蒸汽作为电子供体, 利用可见光催化还原 CO₂, 以 3.87 μmol·g⁻¹·h⁻¹ 的速率高选择性地生成唯一产物 CO。在紫外-可见光辐照下, 表现出更优异的催化活性 (34.39 μmol·g⁻¹·h⁻¹)。经 4 次循环实验, 仍然表现出稳定的光催化二氧化碳还原效率, 证明其具有优异的稳定性。

关键词: 一锅法; WS₂/WO₃ 异质结; CO₂ 还原; 无牺牲剂; 紫外可见光